Evolution in Electrical and Electronic Engineering Vol. 3 No. 1 (2022) 587-597

EEEE

Homepage: http://publisher.uthm.edu.my/periodicals/index.php/eeee
e-ISSN : 2756-8458

Characterization of Electric Field Profile for C_4F_7N with CO_2 Under Different Electrode Configurations

Rizwan Ahmed[1], Rahisham Abd Rahman[1]*, Nur Najihah Abd Latif[1]

[1]Faculty of Electrical and Electronic Engineering,
Universiti Tun Hussein Onn Malaysia, Batu Pahat, 86400, Johor, MALAYSIA

*Corresponding Author Designation

DOI: https://doi.org/10.30880/eeee.2022.03.01.068
Received 20 January 2022; Accepted 30 May 2022; Available online 30 June 2022

Abstract: This research work focuses on the effect of electric field distribution in C_4F_7N dielectric gas under different electrode configurations and varying air gap distances. Finite Element Analysis (FEA) is used to simulate the model in axial-symmetrical. Different electrode configurations such as sphere-sphere, plane-plane, rod-rod, rod-plane, and rod-sphere are utilized to analyze the effect of electric field distribution and breakdown of the proposed gas. It is concluded that the distance between the electrodes significantly impacts the distribution of the electric field in the gap. Shorter the gap distance, the stronger the electric field. The electrode geometry also affects the electric field distribution. The stronger field is observed at the center in sphere-sphere configuration, while in the case of plane-plane configuration, the field intensity is stronger than the sharp edges of the plane electrode.

Keywords: C_4F_7N, Electric Field, Finite Element Analysis (FEA)

1. Introduction

The rapid evolution of technology creates new challenges to environmental protection that could harm our ecosystem. As greenhouse gas emissions blanket the Earth, they trap the sun's heat. This leads to global warming and climate change. The world is now warming faster than at any point in recorded history. The electric power industry plays a key role in the development of a nation and also poses a great threat in terms of transmitting waste byproducts to the environment. Dielectric materials are utilized to insulate high voltage equipment for safe operation. There are three types of insulating materials: gases, solid, and liquid. These materials have different operating conditions and varying conductivity and permittivity [1],[2]. In high and medium voltage operations, the gas insulation has the advantage of being lightweight, construction simplicity, and reduced installation cost compared to solid and liquid insulation. SF6 is extensively used in high voltage equipment due to its excellent dielectric

*Corresponding author: rahisham@uthm.edu.my

properties. Despite its superior insulation characteristic, SF6 is potent greenhouse gas restricted under the KYOTO protocol. The atmospheric lifetime of SF6 is approximately 3200 years and the global warming potential of 23200 relative to CO2. Besides its environmental effect, other factors such as harmful byproducts, corrosiveness, toxicity, and high boiling point argue for restricting its usage.

Many researchers have studied the alternative gases to replace Sf6, and recently Perfluoroisobutyronitrile (C_4F_7N) has been found to be the best substitute. The gas is developed by 3M, which has a dielectric strength more than twice that of SF_6 [3]-[6]. Fundamental knowledge of the insulation characteristics of C_4F_7N gas mixture needs to be analyzed under various conditions.

This research work focuses on the breakdown strength and the electric field stress of C4F7N gas. Different kinds of electrodes and the size of air gaps in the pressure vessel are used to study the electric field strengths. Electrode configurations are selected, namely sphere-sphere, plane-plane, rod-rod, rod-plane, and rod-sphere. Next, the air gap is varied in steps of 0.5 cm, starting from 0.5 cm to 2.5 cm. This work determines the breakdown strength of C4F7N under different electrodes through finite element analysis. The boundary conditions are applied by assigning the relative permittivity and permeability values to every component [7],[8].

Generally, the maximum electric field, E_{max} can be evaluated in each test configuration. Most of the time, the pre-discharge occurs in the region of high stress, where the E_{max} exists. It is complicated to measure the correctly electric field at all locations between two electrodes in the manual calculation. So, in this project, a Finite Element Analysis (FEA) is used for computer simulation. COMSOL Multiphysics software is used to develop the electrode model and analyze the electric field [9,10].

2. Materials and Methods

2.1 Materials

The work is carried out on the dielectric gas C_4F_7N. Table 1 shows the physicochemical properties of C_4F_7N gas. The material properties of test gas, i.e., relative permittivity, are assigned as 2 in simulation software [3].

Table 1: Physiochemical properties of C_4F_7N

Parameters	Values	Unit
Weight (Molecular)	195	g/mol
Density	0.0081	g/cm3
Number of electrons	48	c°
Freezing point	-118	c°
Boiling point at 1 bar	-4.7	M pa
Saturated vapour pressure at -30c°	0.05	M pa
Saturated vapour pressure at 0°	0.15	M pa
Saturated vapour pressure at 20°	0.34	-
Flammability	Non flammable	-
Explosiveness	Non explosive	-
Stable (Chemically)	Inert	-
Stable (Thermally)	Stable up to 700c°	-
Corrosiveness	Non-corrosive	-
Soluble in water	Non-soluble	-
Appearance	Colourless	-
Toxic property	>5000000	-

Different electrode configurations have been used in this work. The sphere electrode has a diameter of 2 cm (radius = 1 cm). The rod electrode has 45° angle with 1.0 cm at the tip. The plane electrode has a radius of 4.5 cm. The electrodes are made from aluminum, categorized as non-sparking metal [4]. It means no spark will be produced in a hazardous environment.

2.2 Method

This project will be carried out based on the flowchart in Figure 1. COMSOL Multiphysics software (5.6) simulates the electric field distribution and hence breakdown characteristics. The simulation software has the advantage of eliminating computational complexities and fast running time. The FEA analysis also measures the breakdown strength and field distribution using software; hence no practical experiments are required, significantly reducing the cost. Pressure vessel with electrodes are designed in the software, then boundary values are assigned, and HV is applied to the HV terminal, and o is applied to the ground terminal. The methodology of this research work is represented in Figure 1.

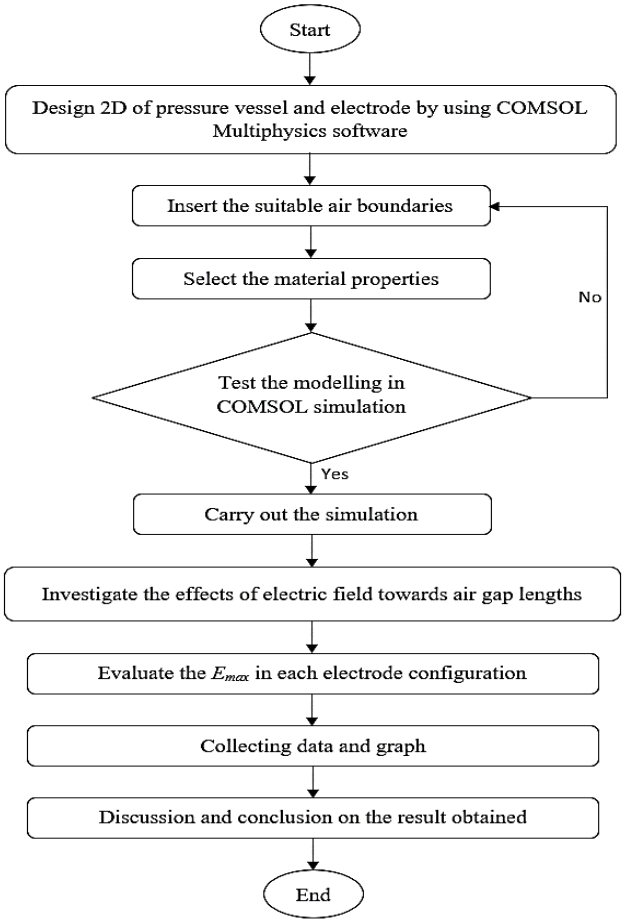

Figure 1: Flowchart of project

The air gap length between the two electrodes is defined as shown in Figure 2. The box is designed with the dimension of 5*5 cm, and the properties of the proposed gas are assigned to it. This is to avoid any influence happening at the box's border along with the air. This box size is ideal because it will have accurate boundary measurements. It also can be a check on the Form Union if there is any dimension over the r-axis ($r < 0$).

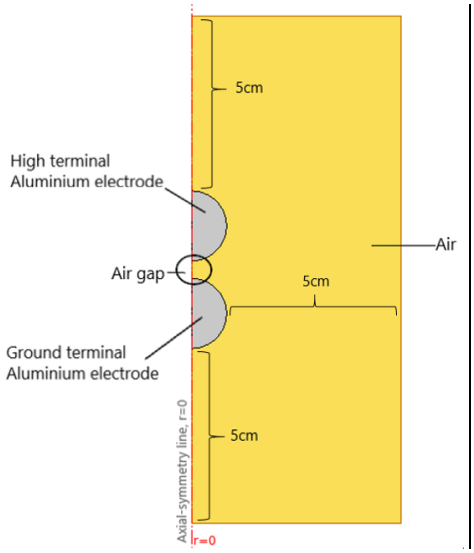

Figure 2: Geometry design of sphere-sphere electrode pair and the bounding box in COMSOL Multiphysics

2.3 Applied Voltage

The maximum applied voltage at the high terminal electrode in the simulation is calculated from the dielectric strength of the dielectric material [5], as shown in Table 2. The formula of maximum voltage that is applied to the electrode is implemented in this process:

$$V_{max} = \text{ED (kV)} \qquad Eq.1$$

Where Vmax (kV), E (kV/cm), D (cm) are the maximum voltage, dielectric strength, and electrodes gap. The dielectric strength value is fixed to 20kV/cm.

Table 2: Physiochemical properties of C_4F_7N

Electrodes gap, D (cm)	V_{max} (kV)
0.5	10
1.0	20
1.5	30
2.0	40
2.5	50

3. Results and Discussion

3.1 Breakdown Strength

The breakdown strength of C_4F_7N under different electrodes configuration is analyzed in FEA software. The electric field strength gives an indication of gas breakdown. The maximum electric field, E_{max} is observed at the rod-plane electrode as compared to the other electrode configurations. The sharp edge of the electrode influences the electric field. The maximum electric field, E_{max} is 2 755 kV/cm obtained in a rod-plane setup which shows this configuration would lead to the breakdown earlier than other tested electrodes setups. The analysis sequence began with rod-plane followed by rod-rod, rod-sphere, plane-plane, and sphere-sphere electrode.

3.2 Electric Field around the electrodes

The electric field intensity is observed based on the color result (known as the contour line) around the electrodes. The color range for the electric field of this simulation is set for all types of electrodes configuration at a range of minimum = 6000 V/cm and maximum = 900000 V/cm. The electric field

along the gap of this simulation is shown in Figure 3 for (a) 0.5cm, (b) 1.0cm, (c) 1.5cm, (d) 2.0cm and (e) 2.5cm for sphere-sphere electrodes. It can be viewed that a 0.5cm air gap has the highest electric field distribution (1785 kV/cm); meanwhile, for 2.5cm air gap has the lowest field distribution due to a larger air gap (750 kV/cm). Additionally, the arrow in Figure 3 shows the electric field's directions that occur around the electrodes where it points from the high terminal electrode to the ground terminal electrode. It shows the strength of the electric field in the air gap and surrounding areas. The arrow direction from the high terminal means the electric field is stronger at that place compared to the ground terminal.

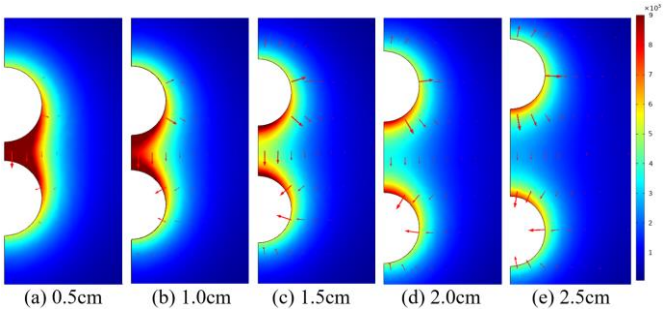

Figure 3: Electric field along the air gap of 0.5cm - 2.5cm

Figure 4 shows the simulation result of electric field intensity from 0.5cm to 2.5cm while maintaining the applied voltage at a high terminal electrode constant at 10kV. As the electrode gap distance increases, the electric field intensity gradually decreases. Vice versa, the shorter the gap distance, the closer the electric field will be. This indicates that the electric field intensity is inversely proportional to the air gap.

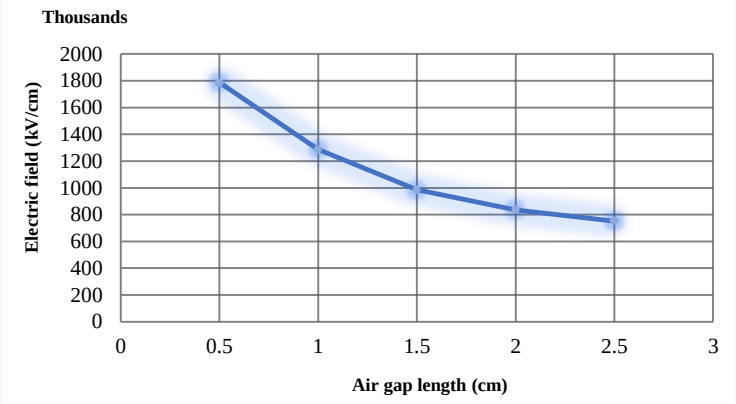

Figure 4: Electric field with 10kV for different electrodes gap

3.3 Electric Field at the X-axis

Figure 5 shows the horizontal line along X-axis that will be analyzed in a graphical chart. The electric field around the electrode is high, indicated by the red contour color measured at 2445 kV/cm. The electric field decreases exponentially from the tip of the high terminal electrode towards the bounding box.

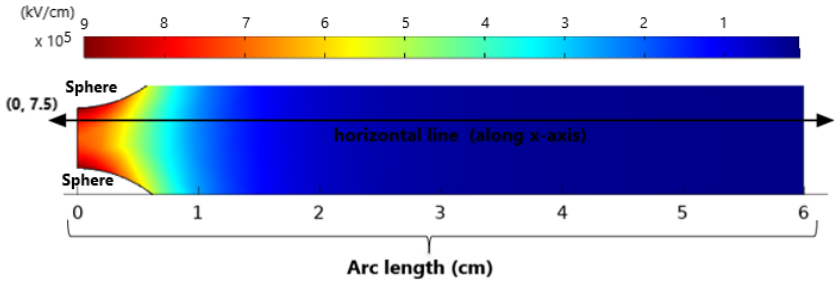

Figure 5: Electric field at the horizontal line along the X-axis

Figure 6 shows the value of the electric field drops as the arc length is nearer to the bounding box. The air gap of 0.5 to 2.5 cm is selected to thoroughly analyze the effect of gap distance on electric field distribution for various electrode configurations. It helps to indicate the maximum differences between the two values, where 0.5cm is the minimum air gap, and 2.5cm is the maximum air gap. This graph proves that the electric field intensity only occurs around the electrodes. This trend graph is similar for rod-rod, rod-sphere, and rod-plane electrodes.

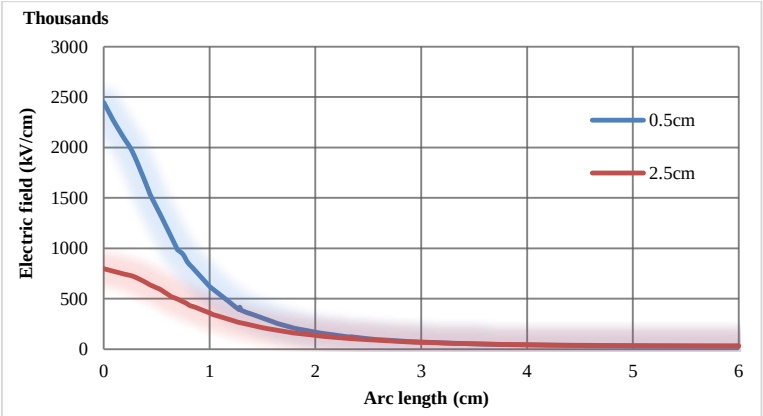

Figure 6: Graphical representation of electric filed along X-axis for 0.5cm and 2.5 cm for sphere-sphere electrode

Meanwhile, the horizontal line along the X-axis for the plane-plane electrode configuration has a different trend. The simulation result shows in Figure 7, where high electric field intensity occurs at the plane electrode's edge. The electric field has a maximum value (892 kV/cm for 1.5cm) in red color at the curve of the electrode compared to sphere-sphere, rod-rod, rod-sphere, and rod-plane electrode configurations. The graph shown in figure 8 is the electric field distribution under plane-plane electrode configuration. The nonlinearity is observed at the center, as seen with the spikes. These spikes arise due to the geometry of the plane electrode, where the higher electric field strength is observed at the side edges of the plane electrodes. The percentage of the spike is shown in Table 3. The greater the value of air gaps between two electrodes, the higher the spike percentage occurs at the edge of the plane electrode.

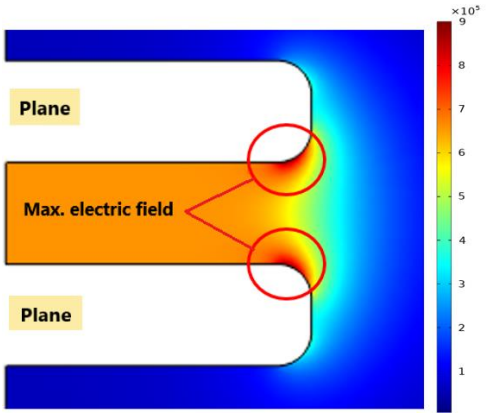

Figure 7: Maximum electric field at the curve of the plane-plane electrode

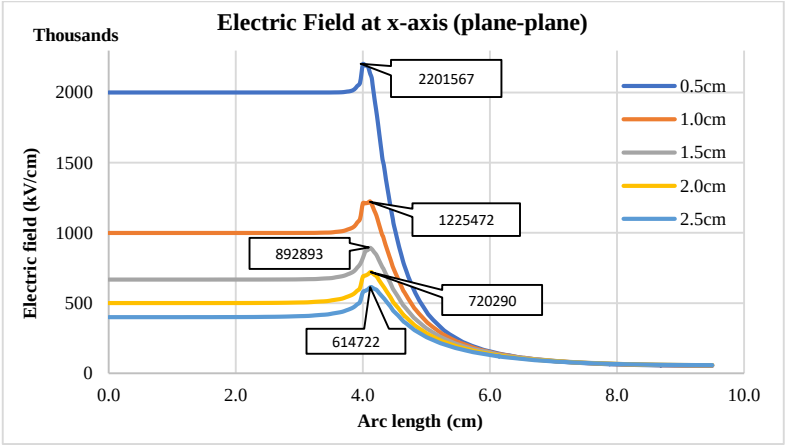

Figure 8: Graphical representation of electric filed along x-axis for 0.5cm-2.5 cm for plane-plane electrode

Table 3: Percentage of the spike at the edge of plane electrode

Air gaps (cm)	% spike
0.5	9.16
1.0	18.40
1.5	25.34
2.0	30.58
2.5	34.93

3.4 Electric Field at Y-axis

As expected, the maximum electric field, E_{max} is located at the tip of the two electrodes between the air gap. Figure 9 shows the position for the minimum point of an electric field at the central point along the Y-axis for the sphere-sphere electrode. Figure 10 shows the trend reaction of a graph is declined in the middle or falls between two neighbouring points. It is stated in the rate of electric field intensity, which is lower at the middle point. This trend graph is also similar for the rod-rod electrode and rod-sphere electrode.

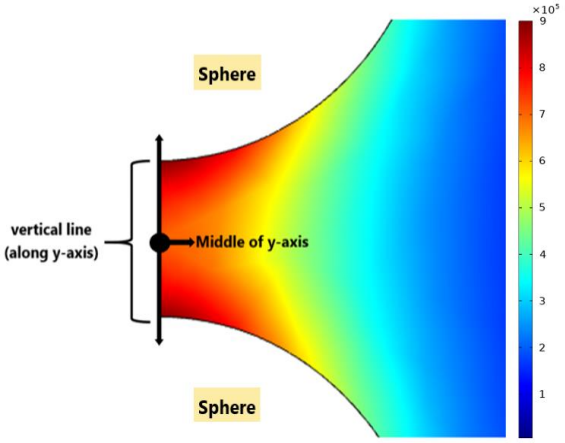

Figure 9: Middle point at the vertical line along Y-axis

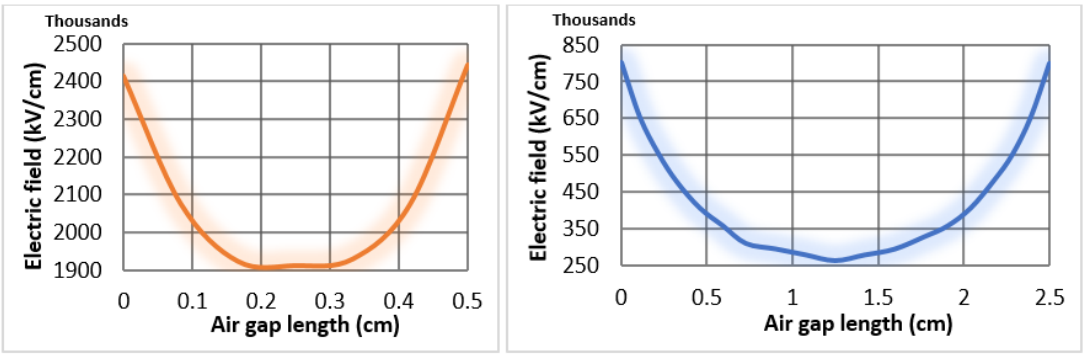

Figure 10: Graphical representation of electric field along the Y-axis for 0.5cm and 2.5cm

These rod-plane electrode configurations have different results, as shown in Figure 11, where the maximum electric field, E_{max} is located at the rod electrode but non at the plane electrode. The electric field occurs at the high terminal of the electrode only. This simulation result shows that the electric field intensity rises when nearer to the high terminal electrode, as shown in Figure 12.

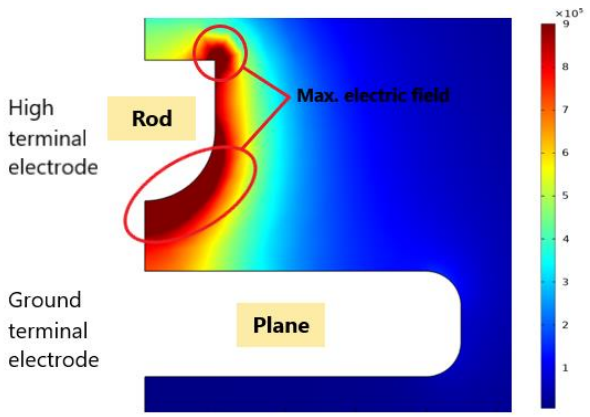

Figure 11: Maximum electric field at the rod electrode

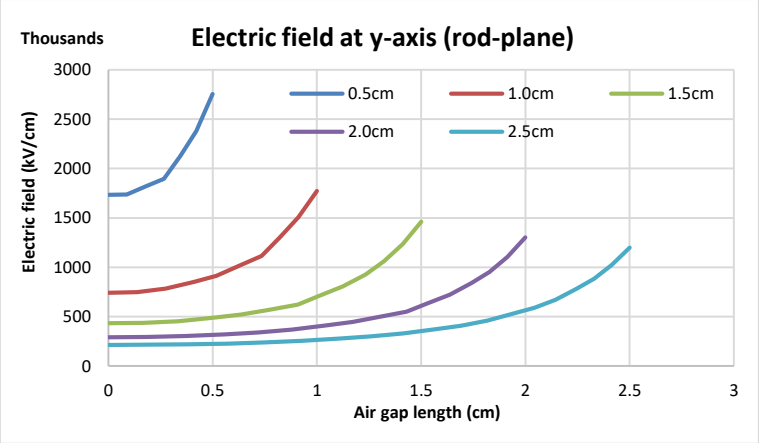

Figure 12: Graphical representation of electric filed along Y-axis for 0.5cm-2.5 cm for rod-plane electrode

Figure 13 shows the selected part of Y-axis for plane-plane electrodes, which is the edge part. The trend shown in Figure 14 is the maximum electric field, E_{max} is identified at the edge of the plane electrodes. The maximum value that has been obtained is 1994 kV/cm.

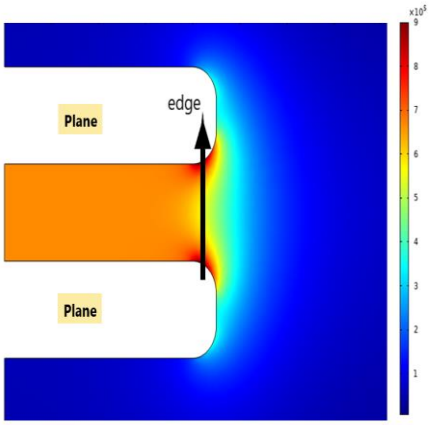

Figure 13: Edge part along Y-axis in a vertical line

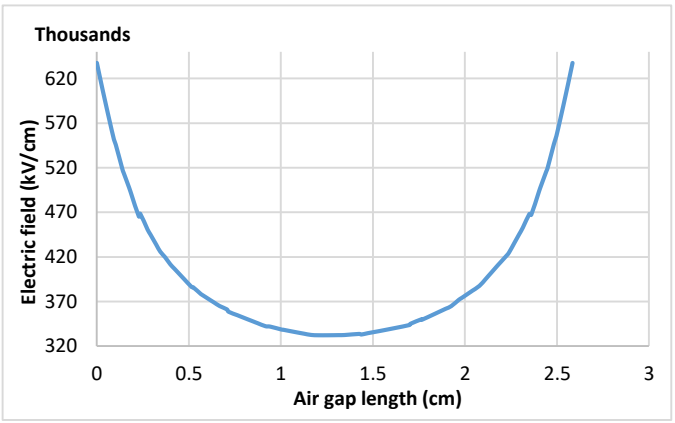

Figure 14: Graphical of electric filed along edge part of Y-axis

The comparison analysis of electric field, E_{max} for different electrode configurations are shown in Table 4. Different electrode configurations have different electric field results even though the air gap and the applied voltage are similar for all the configurations. It can be concluded that the rod-plane electrode configuration has a maximum value of electric field distribution among the other electrode configurations.

Table 4. Comparison of Maximum and minimum electric field strength for different electrode configuration

Electrodes configuration	Maximum electric field strength (kV/cm) at an air gap of 0.5 cm	Minimum electric field strength (kV/cm) at an air gap of 2.5 cm
Sphere-Sphere	1785	750
Plane-Plane	2201	614
Rod-Rod	2379	655
Rod-Plane	2755	450
Rod-Sphere	2373	636

4. Conclusion

FEA tools solve complex computational problems with great accuracy without involving the high cost of experimental work. This study concluded by performing the comprehensive electric field strength analysis of C4F7N in the FEA tool for different electrode configurations as a suitable alternative to replace the SF_6 gas. The applied voltage and air gaps greatly influence the electric field intensity. The simulation result reveals that when the air gap increases, the electric field intensity decreases for all electrode configurations. For rod-plane electrodes, a higher electric field occurs at the high terminal of the electrode only. Besides the plane-plane electrode, a higher electric field intensity is observed at the edge of the plane electrode. Based on the electric field analysis of C4F7N gas, it is concluded that the proposed gas has a huge potential to replace the hazardous SF6 in electrical power applications.

Acknowledgment

This research was made possible by funding from research grant number (FRGS/1/2020/TKO/UTHM/02/6) provided by the Ministry of Higher Education, Malaysia. The authors would also like to thank the Faculty of Electrical and Electronic Engineering, Universiti Tun Hussein Onn Malaysia, for its support.

References

[1] M. S. Naidu and V. Kamaraju, High Voltage Engineering, Second Edi., vol. 15, no. 5. United State: McGraw Hill, 1995.

[2] Sham, N. M. B., N. Z. Zahid, M. S. Kamarudin, N. A. M. Jamail, and R. Abd-Rahman. "Breakdown Characteristic of N2-CO2 Gas Mixtures under AC and DC Test Voltages." In Journal of Physics: Conference Series, vol. 1874, no. 1, p. 012027. IOP Publishing, 2021

[3] R. Ahmad, N. A. M. Jamail, R. A. Rahman, A. A. Rahman, A. A. Salem, and H. A. Hamid, "Finite Element Analysis of Electric Field Distribution in C4F7N as an Alternative to SF6 For Electrical Insulation," IEEE 2021 - 2021 Institute of Electrical and Electronics Engineers, 2021.

[4] Ahmad, R., Khan, F., Jamal, A., Khan, S., Ali, S., Horoub, M. M., & Albalasie, A. (2020, June). Simulation and breakdown characteristics of china clay and silica sand for improved grounding system. In 2020 International Conference on Electrical, Communication, and Computer Engineering (ICECCE) (pp. 1-6). IEEE.

[5] Ahmed, Rizwan, Rahisham Abd Rahman, Arshad Jamal, Ali Ahmed Salem, Bander Saman, Kwan Yiew Lau, and Sherif SM Ghoneim. "Field-Dependent Pollution Model under Polluted Environments for Outdoor Polymeric Insulators." Polymers 14, no. 3 (2022): 516.

[6] B. Khan, J. Saleem, F. Khan, G. Faraz, and N. U. Rehman, "Finite Element Analysis of Electric Field Distribution in the Dielectric Gas R410A as an Alternative to SF6 for High Voltage Applications," ICAEM 2018 - 2018 Int. Conf. Appl. Eng. Math. Proc., pp. 96–101, 2018, doi: 10.1109/ICAEM.2018.8536306.

[7] Ahmed, R., Kim, T., Lee, Y. J., Jeon, S., Yi, J., Choi, I. H., ... & Koo, J. B. (2020). Online condition monitoring and leakage current effect based on local area environment. Transactions on Electrical and Electronic Materials, 21(2), 144-149.

[8] Ahmad, Rizwan, Mahmoud Kassas, Chokri B. Ahmed, Faisal Khan, Sikandar Khan, Arshad Jamal, and Irshad Ullah. "Application of Mineral Compounds for a High-Voltage Portable Grounding System: An Experimental Study." Electronics 10, no. 16 (2021): 2043.

[9] Kamarudin, M. S., N. H. Radzi, A. Ponniran, and R. Abd-Rahman. "Simulation of electric field properties for air breakdown using COMSOL multiphysics." In 4th IET Clean Energy and Technology Conference (CEAT 2016), pp. 1-5. IET, 2016.

[10] Salem, Ali A., Rahisham Abd Rahman, M. S. Kamarudin, and N. A. Othman. "Factors and models of pollution flashover on high voltage outdoor insulators." In 2017 IEEE Conference on Energy Conversion (CENC ON), pp. 241-246. IEEE, 2017.